Chemical Physics Letters 684 (2017) 433–442

Contents lists available at ScienceDirect

Chemical Physics Letters

journal homepage: www.elsevier.com/locate/cplett

Frontiers article

The Jones-Ray effect reinterpreted: Surface tension minima of low ionic strength electrolyte solutions are caused by electric field induced water-water correlations

H.I. Okur [a], Y. Chen [a], D.M. Wilkins [b], S. Roke [a,*]

[a] Laboratory for fundamental BioPhotonics (LBP), Institute of Bioengineering (IBI), Institute of Materials Science (IMX), School of Engineering (STI), Lausanne Centre for Ultrafast Science (LACUS), École Polytechnique Fédérale de Lausanne (EPFL), CH-1015 Lausanne, Switzerland
[b] Laboratory of Computational Science and Modeling, IMX, EPFL, CH-1015 Lausanne, Switzerland

ARTICLE INFO

Article history:
Received 28 April 2017
In final form 9 June 2017
Available online 15 June 2017

Keywords:
Jones-Ray effect
Water
Ions
Interfaces
Surface tension
Second harmonic generation

ABSTRACT

The surface tension of electrolyte solutions exhibits a minimum at millimolar electrolyte concentrations and then rises with increasing concentration. This minimum, known as the Jones-Ray effect, has been hotly debated over the past ~80 years. If not considered as an artifact, it is typically ascribed to a phenomenological rare binding site for ions or ion pairs. Here, we propose an alternative underlying mechanism, namely that the hydrogen bond network of water responds to the collective electrostatic field of ions by increasing its orientational order, supported by recent surface tension measurements of NaCl solutions in H_2O and D_2O, and second harmonic scattering experiments in combination with ion resonant second harmonic reflection experiments. Recent thermodynamic and purely electrostatic treatments of the surface tension provide support for this interpretation. In addition, concerns related to possible artifacts influencing the measurements are quantified experimentally.

1. Introduction

The surface tension of aqueous salt solutions in contact with air generally increases with salt concentration. This increase in the surface tension was first shown and explained, almost 8 decades ago, by Onsager and Samaras with a model based on Debye-Hückel theory [1]. More specifically, the surface tension increases as a result of ion exclusion from the interface that happens as a consequence of electrostatic image forces [1,2]. This surface tension increase as a function of electrolyte concentration is shown in Fig. 1A for a selection of common electrolytes including $BaCl_2$, KI, KCl and NaCl. The data are adapted from Ref. [3]. It can be seen from Fig. 1A that at concentrations > 0.5–1 mol/kg, the surface tension increases linearly. The increase starts in fact already at ~ 50 mM [4]. The slope of the monotonic increase depends on the chemical nature of the electrolyte. This specificity could not be captured by the model of Onsager and Samaras. In recent years, experimental and molecular dynamics simulation studies have shown that there is a specificity in the exclusion of simple ions from the interfaces [5–16]. For instance, ions with high polarizability, i.e., I^-, SCN^-, and Br^-, are less excluded from or even included into the air/water [15,17]. macromolecule/water [10] or oil/water [8,18] interface. Several models have been proposed to explain this ion specificity [5,12,19–26]. What all these explanations have in common, is that the size, polarizability and molecular interactions such as hydrogen bonding and ion-dipole interactions are the main ingredients of the observed behavior. As such, although there remain some open questions, there is a general agreement as to what causes the increase in surface tension. Curiously, such a consensus is not present for ionic strengths below ~50 mM where surface tension measurements have and still are causing controversy.

First, there is the matter of the experimental data. Just one year after Onsager and Samaras introduced their model of ion repulsion at interfaces, Jones and Ray reported on the surface tension of aqueous KCl solution at very low ionic strength. They measured, using the capillary rise method, that the surface tension gradually decreases reaching a surface tension minimum at ~1 mM. Above 1 mM the surface tension gradually increases again according to the above described trend [27]. Fig. 1B displays the data from Ref. [27] for KCl. In subsequent years, using the same method, the same surface tension trend was reported for a total of 13 different electrolyte solutions [28–31]. Jones and Ray showed that all the tested salts have a surface tension minimum near 1 ± 0.5 mM and that the minimum in their measured response corresponded to a change of ~ −0.18‰, a small but reproducible change. The results

* Corresponding author.
E-mail address: sylvie.roke@epfl.ch (S. Roke).

http://dx.doi.org/10.1016/j.cplett.2017.06.018
0009-2614/

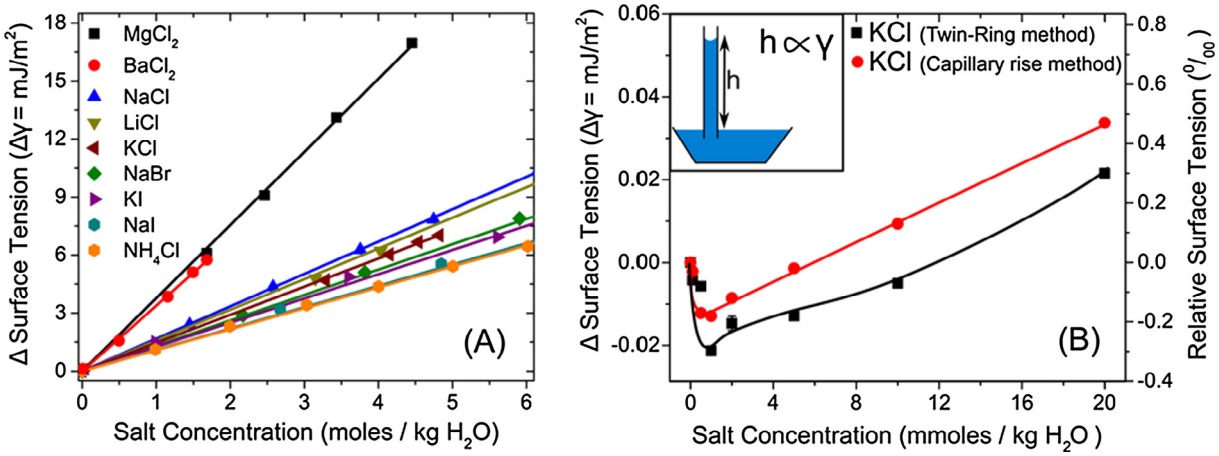

Fig. 1. Surface tension of electrolyte solution in contact with air. (A) Surface tension values of air/aqueous solution interfaces as a function of concentration for various salts as indicated in the legend (adapted from Ref. [3] with permission and fitted with straight lines). Note that the graph does not report on any data points below an electrolyte concentration of 0.5 mol/kg H_2O. (B) Relative change in the surface tension of KCl solution as obtained from the capillary rise method (red circles) by Jones and Ray [27], along with the surface tension values of KCl (black squares) measured with a twin-ring apparatus by Dole and Swartout (adapted from Ref. [32]). The red and black lines are guides to the eye. The inset shows a schematic of the capillary rise method [41]. In this method, the height of an aqueous solution (h) in a thin capillary is proportional to the surface tension ($h \propto \gamma$). All the 13 tested salts by Jones and Ray yield the same trend as the red data set.

by Jones and Ray have been hotly debated: Some researchers have reproduced their results and have proposed an explanation [13–14,32–34]. Others have questioned the validity of the experiments. Langmuir blamed the minimum on artifacts of the capillary rise method, *viz.* the thickness of the wetted film on the glass walls was not well determined [35,36]. Cassel presented an alternative view that an increase of the wetting angle may be involved [37]. Coolidge suggested that the contact angle may be imaginary [38]. In contrast, Dole and Swartout reproduced the Jones-Ray surface tension data with a differential surface tension apparatus, a so-called twin-ring tensiometer, where double 90% Platinum/10% Iridium alloy rings were utilized to measure the surface tension of salt solutions [32]. Another method for measuring surface tension, the bubble pressure method, was employed to measure changes in surface tension. The surface tension decline could be observed, but only with long-lived bubbles. Short-lived bubbles did not show a decrease in the surface tension. This result again raised validity questions, this time about the impact of organic impurities and the influence of atmospheric CO_2(g) in these experiments [39,40].

A second issue is the matter of the underlying mechanism. Why would the surface tension have a minimum at very low ionic strengths and why is this not ion specific? Dole was the first accepting the validity of the experimental results by Jones and Ray and suggested a mechanism that is based on the adsorption of ions to a phenomenological and exceptional binding site (in his own wording 'active spot') on the water surface [42].

Since surface tension measurements report on free energy changes that are not specific to any of the constituents of the system or to any mechanism, a more surface specific probe is needed. A decade ago, Koelsch and Motschmann performed ellipsometry measurements on salt solutions [43–45]. They quantified their method and calibrated their instrument against surface tension and second harmonic generation (SHG) of ionic dye solutions, and determined that their experiment would be sensitive enough to detect the minute amounts of ions in the interfacial region that are necessary to reduce the surface tension. However, no change in the ellipsometric response was found below 10 mM. (P. Koelsch, private communication 'I thought by that time that we should be able to see ion induced differences in the ellipsometric angle Δ, but it stayed dead flat.') Around the same time, Petersen and Saykally reported ion resonant SHG surface reflection experiments that showed an increase in the SHG response at concentrations ~ 0.5 mM and saturating at ~ 100 mM [13,14]. The resulting intensity change as a function of salt concentration followed the shape of a Langmuir isotherm. It was therefore concluded that ions bind to specific surface sites already at very low salt concentrations. The mechanism for this behavior was essentially identical to that of Dole using the same phenomenological rare binding site argument. After all, at very low ionic strengths ions are preferably solvated, as the hydration free energy of most ions are negative and thus, favorable. Recently, Garde and coworkers suggested that such a rare binding site could involve the pairing of ions with the counterions being situated at the interface [34], even though this should happen at very low ionic strengths where ion pairs have not been observed experimentally. Overall, the Jones-Ray effect has been considered as a surface phenomenon and the suggested mechanisms involve a rare, unknown ion or ion pair binding site. This non-ion specific binding site that saturates around a few mM salt concentration is hard to reconcile with physical arguments and thus many researchers have been, and still are, questioning the Jones-Ray effect and its explanation [13.14,29,31,33.34,37–40].

In this work we revisit a recent reproduction of the Jones-Ray effect [33], measured with the Wilhelmy plate method for NaCl in H_2O and D_2O (Fig. 2A). We first discuss the interpretation of a surface tension measurement using the Wilhelmy plate method and then examine the abovementioned experimental concerns in detail, considering the contact angle, the effect of dissolved CO_2(g) and the influence of organic impurities by means of explicit measurements. We then consider the interpretation starting from thermodynamic expressions and discuss possible mechanisms behind the Jones-Ray effect based on bulk specific and surface specific second harmonic measurements. These measurements show changes for light and heavy water that match the difference observed in the surface tension measurements, and paint a picture of the reorientation of (bulk) water in the extended hydration shells being responsible for the observed decrease in surface tension, rather than filling up of surface binding sites. Thus, instead of the electrolytes being attracted by the interface to a rare binding site, it is the bulk solution that is responsible for the observed effect. We finish with a discussion of two recently published thermodynamic and purely electrostatic treatments of the surface tension that support this interpretation.

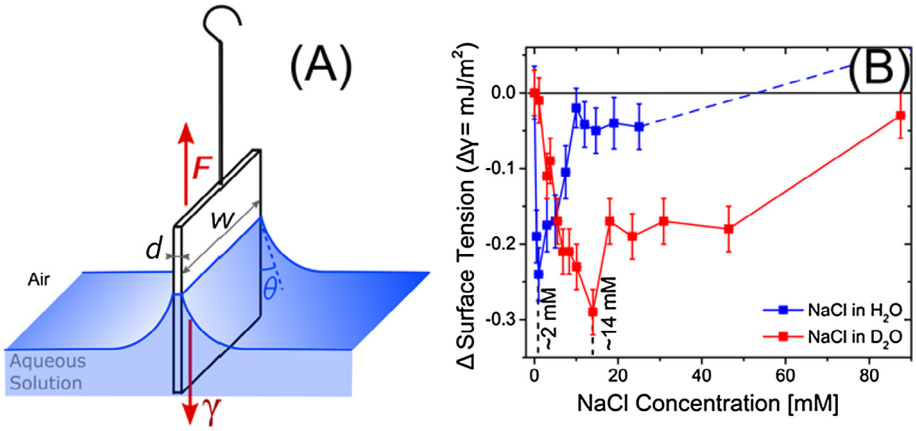

Fig. 2. Wilhelmy plate surface tension measurement. (A) Illustration of the Wilhelmy plate method. (B) Surface tension difference ($\Delta\gamma$) is measured as a function of NaCl concentration for solutions in H_2O (blue) and in D_2O (red). The red and blue lines connect the data points and the dashed blue line indicates the surface tension increase based on the slope of NaCl data in Fig. 1A.

2. Materials and methods

2.1. Chemicals

All chemicals that were employed for the different measurements were used as received. A NANOpure Ultrapure Water System (Barnstead) and a Milli-Q-UF-Plus instrument (Millipore Inc.) were employed to obtain 18.1 MΩ cm water to prepare light water (H_2O) samples. All heavy water samples were prepared with D_2O (99.9% d, > 2 MΩ cm, Cambridge Isotope Laboratories and Armar) Samples were prepared in glassware that was piranha (3:1 H_2SO_4 (95–98%, Sigma) and H_2O_2 (30%, Macron Fine Chemicals)) cleaned and rinsed with copious amounts of ultrapure water prior to use.

2.2. Surface tension measurements

Surface tension measurements were performed using the Wilhelmy plate method. The Wilhelmy plate method [41], as illustrated in Fig. 2A, uses a vertically suspended Pt plate with a perimeter (l) which is pulled out of the electrolyte solution towards the air. The force (F) acting on this plate is measured with a microbalance, and it is correlated to the surface tension (γ) by the following equation:

$$\gamma = \frac{F}{l\cos(\varphi)} \tag{1}$$

Here φ is the contact angle between Pt and water. φ is assumed to have a value of $\varphi = 0$ based on literature [46]. This is verified in Fig. 3. With $\varphi = 0^{\circ}$ the measurement accuracy of the method is ~0.1% [41].

The surface tension (γ) can be defined as the change in the free energy when the surface area is increased by a unit area [41]. For an air (a)/water (w) interface it can be expressed by:

$$\gamma = \frac{1}{2}W_w + \frac{1}{2}W_a - W_{wa} \tag{2}$$

W_w and W_a are the reversible work needed to separate two unit areas of two surfaces from contact with one another to infinite spacing in vacuum. W_{wa} refers to the work of adhesion to create a unit area of air and water. Since molecules in an ideal gas are non-interacting $W_a \to 0$. $W_{wa} \to 0$ as well because of the low concentration of gas molecules compared to the concentration of water molecules in the liquid phase (a factor of 1000 lower). The change in the surface tension in Fig. 2B, $\Delta\gamma$ ($\Delta\gamma = \gamma_{solution} - \gamma_{water}$), as a function of electrolyte concentration can be expressed as:

$$\frac{\partial\Delta\gamma}{\partial c} = \frac{1}{2}\frac{\partial\Delta W_w}{\partial c} + \frac{\partial\Delta W_a}{\partial c} - \frac{\partial\Delta W_{wa}}{\partial c} = \frac{1}{2}\frac{\partial\Delta W_w}{\partial c} \tag{3}$$

Since $W_a \to 0$ and $W_{wa} \to 0$, $\frac{\partial\Delta W_a}{\partial c} = \frac{\partial\Delta W_{wa}}{\partial c} = 0$.

To measure small changes in the surface tension, care needs to be taken because of the possibility of surface active contaminations. To help eliminate this effect, all solutions were stored in closed glass containers with glass caps as opposed to plastic or Teflon ones. The glassware was cleaned in a piranha solution (3:1 H_2SO_4:H_2O_2) before use. Moreover, sample solutions were freshly prepared just prior the measurement with degassed ultrapure water or D_2O and with different batches of highly pure NaCl salt (>99.999%, the highest commercially available). Environmental influences including any possible dust contamination, vibrational instability, and temperature were maximally minimized: The experiments were performed in a class 1000 clean room (ISO class 6, 1000 p/ft^3, Clean Air Products), with an Attension Sigma 701 Force Tensiometer (Biolin Scientific), that is equipped with an Attension Pt Wilhelmy plate (Biolin Scientific). This apparatus was placed on a vibrationally isolated table (Micro-g Lab Table, TMC). The room temperature was monitored and controlled to stay within 23.5 ± 0.3 °C over the course of the experiments. Moreover, personal protective equipment including nitrile gloves, a hair net and clean room compatible garments were worn at all times. The Pt Wilhelmy plate was cleaned with a flame produced by a mixture of H_2:O_2 gas in order to make sure the Pt surface is kept clean from any organic impurities including unburned organic gas molecules. In a generic measurement, the aqueous solutions were measured with 40 mL of desired aqueous solution in a glass crystallization dish that has 102 cm^2 surface area in contact with ambient clean room air. Each sample solution was probed a minimum of 40 times (~40 min) and every reported surface tension data point was reproduced at least 5 independent times for H_2O and 2 times for D_2O.

2.3. Contact angle measurements

The contact angle measurements were performed with a Drop-shape analyzer (DSA 30, Krüss). A schematic of the experimental setup is illustrated in Fig. 3A. In these measurements, a freshly cleaned Attension Pt Wilhelmy plate (Biolin Scientific) was placed vertically on the sample stage. Then, we placed 30 μL of aqueous solutions at various NaCl concentrations on the side surface of the Pt Wilhelmy plate and the resultant droplet shape was acquired. The contact angle value was detected by the ADVANCE software (Krüss) unless a complete wetting occurs. When the drop

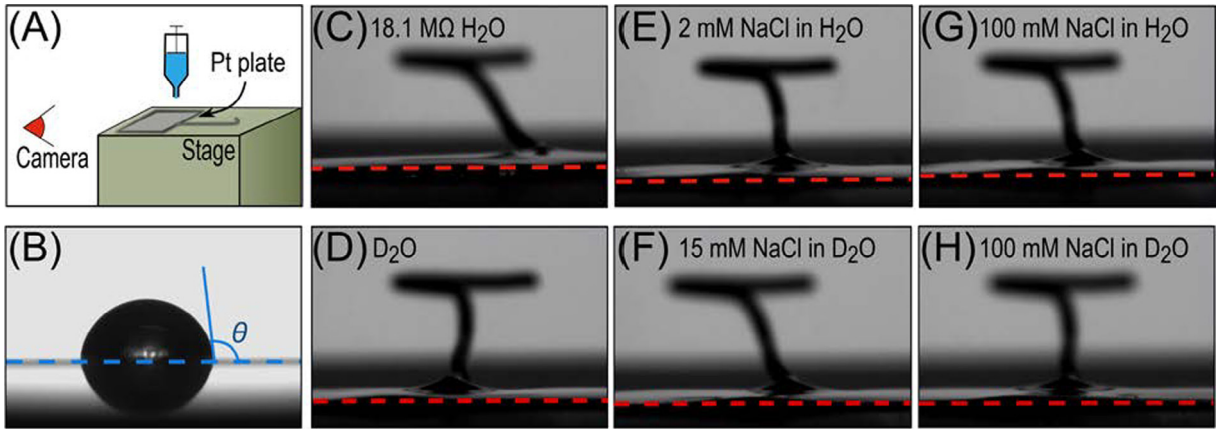

Fig. 3. Contact angle measurements. (A) Illustration of the experimental setup for contact angle measurements. (B) Contact angle (Θ) measurement of a polyethylene surface. Here $\Theta = 95°$. (C)–(H) Snapshots of a freshly cleaned Pt Wilhelmy plate exposed to 30 μL of various solutions: (C) ultrapure H_2O, (D) D_2O, (E) concentrations close to the surface tension minimum: 2 mM NaCl in H_2O, (F) 15 mM NaCl in D_2O, and concentrations well beyond the minimum: (G) 100 mM NaCl salt solution in H_2O, (H) 100 mM NaCl in D_2O. In all these figures the added solutions completely wet the metal surface and water droplets cannot be seen. The out of focus feature is the hook of the Wilhelmy plate, (see Fig. 2A). The red dashed lines denote the position of the Pt surface and the blue dashed line indicates the polyethylene surface.

completely spread over the substrate surface, the contact angle was considered to be 0° [41]. Note that, all tested sample solutions demonstrated complete wetting properties when the Pt plate was utilized as a substrate. The contact angle of a polyethylene/aqueous solution interface was also acquired as a reference sample, yielding a contact angle of 95° [47].

2.4. Total organic content measurements

The amount of organic impurities in tested aqueous solutions was acquired with a total organic content analyzer (TOC-V, Shimadzu), that has a detection limit of 0.5 μg/L. First, a reference aqueous sample with 10 μM concentration of sodium dodecyl sulfate (SDS) surfactant was measured in which the total amount of organic content was reported to be 10% more than the added SDS amount. This degree of error is expected based on the above-mentioned detection limit of the instrument. In order to test the organic impurity in the aqueous salt solutions, a 4 M NaCl (99.999%, Sigma-Aldrich) salt solution was analyzed. Such a high salt concentration is necessary to reliably detect the trace amount of organic impurity contained in the salt, if there is any.

2.5. Conductivity and pH measurements

The pH and conductivity of aqueous solutions were obtained with potentiometric measurements. A Henna Multimeter (HI-5521, Henna Instruments, USA) capable of performing both pH measurements (using a glass electrode HI 1131, Henna Instruments) as well as conductivity measurements (using a Pt wire conductivity probe HI-36312) was employed. The pH meter was calibrated before measuring with standard pH solutions of pH 4.01, pH 7.01, and pH 10.01 (Henna Ins.; HI-7004, HI-7007, and HI-7010). The pH measurements were performed with two separate pH electrodes, and the data are recorded after the readout value remains unchanged at least for a few minutes. The reported hydronium ion concentration ($[H^+]$) of the tested solutions are calculated from the measured pH values with the following expression: $[H^+] = 10^{-pH}$.

The conductivity meter was also calibrated before the reported measurements with standard solutions of 84 μS/cm, 1413 μS/cm, and 12,880 μS/cm (Henna Instruments; HI-7033, HI-7031, and HI-7030). At low ionic strength, a bottle of 84 μS/cm standard solution was freshly opened for every calibration to eliminate possible errors in the calibration of the instrument. Nevertheless, the error in the conductivity measurements is around 3% of the readout value. The conductivity is associated with the mobility of the ions in aqueous solution. As such, H^+ ions have a ~ 6 times higher conductivity (36.23×10^{-8} m^2 s^{-1} V^{-1} @ 298 K) compared to Na^+ and Cl^- (5.19×10^{-8} and 7.91×10^{-8} m^2 s^{-1} V^{-1} @ 298 K) [48]. In other words, 1 μM carbonic acid (NaCl) formation corresponds to an ~0.43 μS/cm (~0.13 μS/cm) increase in conductivity. The sample solutions were prepared at 27 μM and 2.5 mM of NaCl (99.999%, Sigma-Aldrich) in H_2O. The stock solutions were separated into 15 mL portions in open containers with 9.3 cm^2 air/water surface area. For the conductivity and pH measurements, the area in direct contact with ambient air per volume of solution per time was kept identical to the surface tension measurements in order to be able to make a valid comparison (shown as the yellow highlighted region in Fig. 4A and B).

2.6. Resonant second harmonic generation

The details of the experiments can be found elsewhere [11,13,14]. The resonant second harmonic data are adapted from Refs. [14,33]. Briefly, a homebuilt femtosecond oscillator was employed to pump a regenerative amplifier (Spectra Physics, Spitfire, 1 kHz, 90 fs, 2 mJ) after which two optical parametric amplifiers (Light Conversion, TOPAS) enables tunability. The fundamental laser beam was focused onto the sample solution at 45°. The reflected second harmonic light was filtered and recollimated with dichroic mirrors, and prism. Then, it was collected with a solar blind PMT (Hamamatsu, R7154PHA). The sample solutions were gently stirred by flowing nitrogen over the sample solution. Each data point was reproduced over at least 2 different days.

2.7. fs-Elastic second harmonic scattering measurements (fs-ESHS)

The details of our fs-ESHS setup [49] and the details of bulk aqueous solution experiments [33] were described and discussed in details elsewhere. Briefly, a beam of 190-fs laser pulses centered at 1028 nm at 200-kHz repetition rate was filtered (FEL0750, Thorlabs) and employed as the fundamental beam with 0.3 μJ pulse energy (incident laser power P = 60 mW). The polarization of the input pulses is controlled by a Glan-Taylor polarizer (GT10-B, Thorlabs), and zero-order half-wave plate (WPH05M-1030). The input pulses were focused into a cylindrical glass sample cell (inner

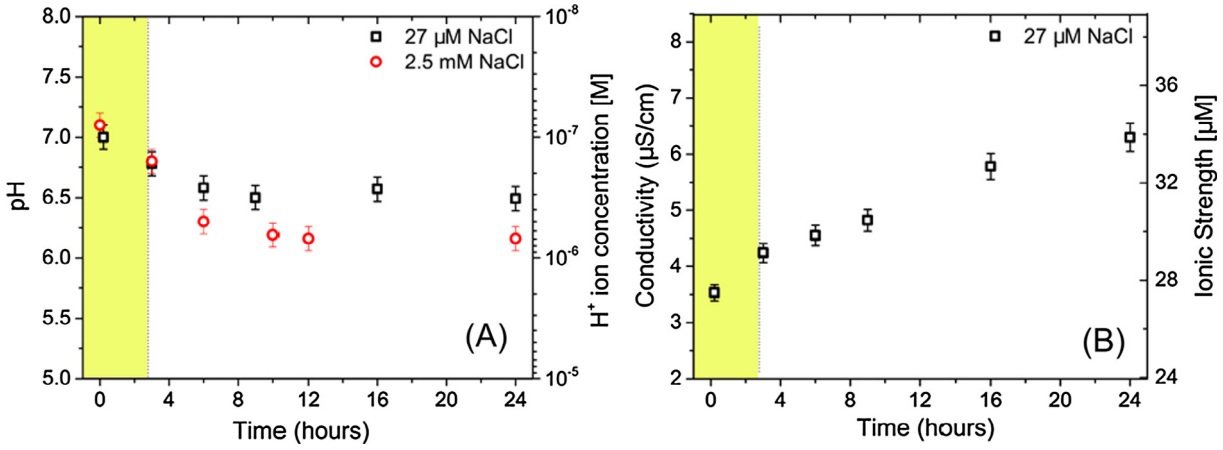

Fig. 4. pH and conductivity measurements of aqueous solutions in contact with air. (A) The pH (left) and H^+ ion concentration (right) for 27 μM NaCl (black squares) and 2.5 mM NaCl (red circles) salt solution as a function of time in hours. (B) The conductivity (left) and ionic strength (right) of 27 μM NaCl in H_2O as a function of time. Both figures show data for aqueous solutions kept in contact with ambient air. Note that, the conductivity readout of 2.5 mM NaCl salt solution was 540 μS/cm. The changes due to carbonic acid formation are insignificant for that case (data not shown). The yellow region in both graphs highlights the maximum duration of the surface tension measurement of a single solution (see Materials and Methods section).

diameter, 4.3 mm) with a waist diameter ~35 μm and a Rayleigh length of 0.94 mm. The scattered second harmonic light was collected with a plano-convex lens (f = 5 cm), then filtered and polarized with optical elements (ET525/50, Chroma) and (GT10-A, Thorlabs), respectively. Finally, the SH scattered light was focused into a gated photomultiplier tube (H7421-40, Hamamatsu). The detection angle was fixed to 90° with an acceptance angle of 11.4°. The data points were acquired with an acquisition time of 1 s × 50 and gated width of 10 ns. The fs-ESHS signal of pure H_2O and D_2O samples was measured as a reference between every two sample measurements. The reproducibly of the fs-ESHS measurements was 1–3%. The sample solutions were prepared with the highest purity salts NaCl (99.999%, Acros) and NaI (99.999%, Sigma-Aldrich) that were measured and stored in sealed glass sample cells. The stock solutions were filtered (Millipore Millex-VV 0.1 μM polyvinylidene difluoride membrane filters) and diluted to the desired ionic strength solutions.

3. Results and discussion

Fig. 2B shows the change in surface tension ($\Delta\gamma$) as a function of NaCl concentration in H_2O (blue) and in D_2O (red) as measured with the Wilhelmy plate method (illustrated in Fig. 2A). It can be seen that for both H_2O and D_2O, the surface tension (γ) decreases at low electrolyte concentrations. For NaCl in H_2O there is a minimum near 2 ± 1 mM ($\Delta\gamma = -0.24$ mJ/m^2), and this depressed region has a width of 10 to 20 mM. The minimum in surface tension occurs at ~ 14 mM ($\Delta\gamma = -0.29$ mJ/m^2) for D_2O and this shallow minimum is even broader than for H_2O. These observations thus confirm that small changes in the surface tension of dilute salt solutions can be measured. Moreover, the minimum in the surface tension of the H_2O/air interface appears at the same concentration range as in the measurement of Jones and Ray. D_2O solutions, on the other hand, display a minimum at a very different (~14 mM) but still low concentration. This difference suggests that the solvent plays a major role (rather than the ion, as in the high concentration range) in determining the free energy difference between the surface and the bulk.

Before discussing a possible mechanism that explains the influence of the solute on the surface tension in detail with the aid of SHG experiments of both the water and the ions, we first discuss and consider concerns about the experiments performed on low salt concentration aqueous solutions, considering the different surface tension measurement methods, the contribution of a possible non-zero contact angle of the Pt/water interface, the presence of organic impurities, and the effect of dissolved CO_2(g) and ions from the walls of the glass container. The following results and discussion section is therefore divided into three sections:

(I) A quantification of possible experimental artifacts that could influence the Jones-Ray effect.
(II) A discussion of the results of SH reflection and scattering experiments that are used to probe the interface and the bulk of aqueous electrolyte solutions. This section is subdivided into observations concerning the surface, the bulk as well as their interpretation.
(III) A discussion of the connection between the second harmonic measurements and the surface tension, and a subsequent proposed mechanism.

3.1. Experimental issues related to the Jones-Ray effect

3.1.1. The difference in the absolute decrease of the surface tension values between various measurements

The magnitude of the change in γ, ~0.5%, is bigger than the change observed by Jones and Ray. The difference can be explained as follows. With the Wilhelmy plate method (Fig. 2B) the air/water surface tension is measured directly and relates only to the work of adhesion of the air/water interface. The capillary rise method used by Jones and Ray (inset, Fig. 1B) also reports on changes of the glass/water interface (which has a non-zero contact angle of ~20–30° depending on the surface pretreatment [50]), and the measured changes in the height of the water column also correlate non-trivially to changes in the thickness of the water meniscus (r) [35]. The magnitudes measured by the capillary rise method are therefore always smaller than those measured by the Wilhelmy plate method [41]. The data measured with the Pt/Ir ring balance method [32] (also shown in Fig. 1B) displays indeed a larger change in the surface tension, but it is still smaller than what we measured in Fig. 2B. This difference is explained by the water used: distilled vs. ultrapure water. The distilled water used in the 1930s and 1940s probably has a significantly higher ionic strength (>100 μM) than the ultrapure water of today (<1 μM), which would reduce the relative change observed in the surface tension.

3.1.2. The contact angle of the Pt Wilhelmy plate with water

Embedded in Eq. (2) there is the assumption that the contact angle φ between Pt and H_2O and D_2O or their corresponding salt solutions is 0°. In that case, the force that is measured in Eq. (1) relates only to the work of adhesion (W_w) term of the air/water interface in Eq. (2) and not to any effects arising from Pt/water interactions. This assumption can be directly verified by contact angle measurements. A schematic of the experimental apparatus is illustrated in Fig. 3A. Fig. 3 B–H show contact angle measurements for water on polyethylene (3B) and on the Wilhelmy Pt plate in contact with H_2O (3C), D_2O (3D), 2 mM NaCl in H_2O (3E), 15 mM NaCl in D_2O (3F), 100 mM NaCl in H_2O (3G) and 100 mM NaCl in D_2O (3H). It can be seen in Fig. 3B that the measured contact angle of the polyethylene/water interface is 95°, in agreement with the literature [47]. It can also be seen that for all aqueous solutions in contact with the Pt Wilhelmy plate, the contact angle is 0°. This means that our Pt plate is completely wetted, in agreement with the literature [46]. It also shows that adding salt or changing H_2O to D_2O does not change the contact angle. These measurements validate that the reported force per area as measured with a Pt Wilhelmy plate (Fig. 2 and Eq. (1)) is equal to the surface tension value of the air/aqueous solution interface.

3.1.3. The presence of organic impurities in salt

A commonly raised concern for surface tension measurements or in general for any air/water interface measurement performed at low ionic strength is the influence of trace organic impurities in the main phase on the surface properties. Trace impurities might lower the interfacial tension as they are generally surface active, and surface active agents are known to lower the surface tension up to a concentration range of 10–100 mM [51], depending on the critical micelle concentration (cmc). At concentrations above the cmc the surface tension remains constant at a very low value. To determine the magnitude of this effect, we measured the concentration of organic contaminants in NaCl solutions with a total organic content (TOC) analysis. To determine the TOC in the electrolyte solutions we measured the TOC of 4 M NaCl salt solutions. We found an average value of 1.33 ± 0.15 mg/L of organic impurity content. Assuming an average molecular weight of 200 g/mol for a hypothetical organic impurity, the concentration of organic impurity in a 4 M NaCl solution would amount to 6.5 μM. Then, for a 2 mM NaCl solution, this analysis would bring the concentration of organic content down to 3.3 nM. Assuming now that those impurities are also surface active, they should have a cmc in the range 10 μM–100 mM [51]. With 3.3 nM being far below the cmc, and the observation comprising a minimum, from which the surface tension rises again, it cannot be expected that organic impurities will lead to the observed surface tension changes in Fig 2B. Moreover, since cmc's are only barely different in light and heavy water [52], we would not expect a difference in the surface tension of light and heavy water for organic impurity induced surface tension changes. As such, the influence of organic contaminants is only minimal and cannot account for the observed surface tension minimum of the Jones-Ray effect.

3.1.4. The influence of CO_2(g) from ambient air

Another possible source of artifacts is the total amount of dissolved CO_2(aq) in the aqueous solution. The equilibrium between atmospheric CO_2(g) and water acidifies the aqueous solutions via carbonic acid formation, leading to changes in the ionic strength. In order to probe solution acidification, we performed pH and conductivity measurements of aqueous NaCl solutions. Fig. 4A shows pH measurements (left axis) for 27 μM and 2.5 mM NaCl solutions and corresponding H^+ ion concentration (right axis). The solutions were prepared in containers in contact with ambient air. Fig. 4B shows the total conductivity (left axis) and calculated ionic strength (right axis) for a 27 μM solution of NaCl in contact with ambient air. The pH (red circles and black squares, Fig. 4A) of the aqueous solutions gradually decreases and the conductivity (Fig. 4B) gradually increases as a function of time. For both solutions, indeed, the pH of the solution alters as a function of time. Nevertheless, the corresponding changes are very small, amounting to an increment in the hydronium concentration of 4×10^{-7} (27 μM), and 8×10^{-7} (2.5 μM) after 24 h. The conductivity increase for the former solution amounts to 6.2 μM of added ions after 24 h. As the surface tension measurements were performed on fresh solutions and took no more than 1 h, as indicated by the yellow area, the effect of carbonic acid from the atmosphere, or the desorption of ions from the walls of the glass containers results in a maximum increase in the ionic strength of 1.4 μM. It can thus be excluded as being of significant influence for the Jones-Ray effect. In addition, the pK_a value for the H^+ ion formation from dissolution of CO_2(g) is different in light and heavy water ~5.65 vs ~6.10, respectively [53,54]. With such a difference, if there was any significant effect from CO_2(g) on our surface tension data, the minimum in D_2O would have to appear at lower concentrations, not at higher ones.

3.2. Probing the surface and the aqueous phase with second harmonic generation

3.2.1. The surface

The adsorption of ions on the air/water interface was probed with resonant SHG experiments by the Saykally lab [13,14]. In these experiments, the second harmonic wavelength was tuned to match the energy of the charge transfer to solvent transition of certain anions. As such, the SHG photons probe the surface presence of anions in the first monolayers of the interface. The thickness of this slab is not well defined, however, as it is determined by a criterion of absence of spatial centrosymmetry of the anions [55]. The resonant response of I^- ions in NaI and KI solutions is plotted in Fig. 5A. As can be seen, the resonant second harmonic ion response starts to rise at ~0.5 mM and levels of at ~100 mM for both NaI (orange squares) and KI (green circles). Beyond hundreds of mM salt concentration, it increases again [13]. The found trend directly indicates the accumulation of I^- ions to the air/water interface. This data was described in terms of surface binding sites, as the curve matches a Langmuir adsorption isotherm.[13] Based on this assumption, the ΔG of adsorption was determined to be −6.1 kcal/mol (−25.5 kJ/mol or −10 kT). This is a very large free energy of adsorption, and one that easily competes with the strength of hydrogen bonds. What type of binding site would have to be responsible for this behavior is not clear. Also, interestingly, comparing the data of Fig. 2B with that of Fig. 5A, we can see that the minimum of the surface tension does not coincide with the saturation of the resonant SHG response. The minimum in $\Delta\gamma$ is reached at ~ 0.2 × the SHG intensity saturation. Compared to well-known binding behavior of surfactants a leveling-off of the resonant SHG response should coincide with the lowest surface tension, which should remain constant at higher concentrations [56]. Both of these observations complicate the interpretation in the surface tension minimum in terms of a surface binding site.

3.2.2. The bulk

More recently, a non-resonant optical experiment, femtosecond Elastic Second Harmonic Scattering (fs-ESHS), was shown to report on the orientation order of water molecules in solution [33,49]. Using this method, an ion induced increase in the orientational order of water molecules was found in 21 different electrolyte solutions. For every salt solution, the response was identical with increasing ionic strength. Fig. 5A shows the fs-ESHS response from the bulk solutions for NaI (purple squares) and NaCl (blue circles)

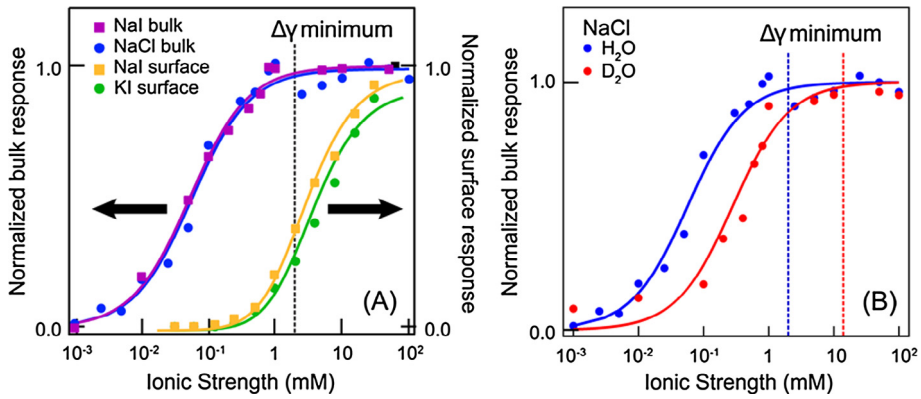

Fig. 5. Molecular level information from the surface and bulk phase. (A) Normalized fs-ESHS intensity (left axis, normalized bulk response) from bulk NaI (purple squares) and NaCl (blue circles) solutions along with the normalized SHG ion resonant interfacial response (right axis, normalized surface response) for NaI (orange squares) and KI (green circles) aqueous solutions plotted as a function of ionic strength. The arrows indicate the designated axis for the corresponding data set. The ion resonant interfacial response is adapted from Ref. [33]. (B) The normalized fs-ESHS intensity obtained in the PPP polarization combination of a NaCl salt solution as a function of salt concentration in H_2O and in D_2O. This data is normalized with respect to the response of bulk ultrapure water (H_2O or D_2O) and scaled such that they are of equal intensity (to compare the shift in concentration; the D_2O response has ~1/3 of the intensity change of the H_2O response [33]). The vertical dashed lines indicate the ionic strengths where the surface tension minima occur in H_2O (blue) and in D_2O (red).

salts as a function of ionic strength. As can be seen, the bulk response shows a trend similar to the surface response, but the curve is shifted to significantly lower salt concentrations, by approximately three orders of magnitude. The fs-ESHS intensity starts to rise at 5–10 μM, and saturates at ~1–2 mM. This data clearly indicates that adding electrolytes to water results in a noticeable increase in the orientational alignment of water. Such an increase is not specific to the type of ion and occurs already at very low concentrations, indicating that the orientational ordering must be longer range than the first few hydration shells where ion-water interactions are specific [5,57–61].

3.2.3. Interpretation

The observed fs-ESHS intensity change as a function of electrolyte concentration appears in the PPP and PSS polarization combinations and not in the SSS and SPP polarization combinations [33]. The intensity changes, therefore, arise from the water and not from the ions. That this is so can be inferred from the following experimental observations: First, based on the selection rules for SHG [62], changes in the intensity in the PPP/PSS polarization combinations, but not in the SSS/SPP polarization combinations, point towards structural correlations. This structural correlation must originate from orientationally correlated molecules that are themselves non-centrosymmetric and have some kind of spherical symmetry in their orientational distribution. Therefore, all centrosymmetric (spherical) ions are excluded as a source of the intensity change observed in the PPP response of Fig. 5. If the intensity increase was dominated by single ions, the response would be present in all 4 polarization combinations. In addition, neither uncorrelated ions at low concentration nor correlated ions at high concentration are likely to have a spherical symmetry in their spatial distribution. Furthermore, pure H_2O and D_2O differ in their coherent responses (Ref. [33], Fig. S5, supplementary material).

It is also apparent from the fs-ESHS data that the underlying structural correlations must occur over longer distances than the first 1–3 hydration shells. If the intensity changes were to come from water that interacts with ions over a short-range via ion-dipole interactions, then we should have observed ion specificity (as in Fig. 1A). Fig. 5B shows that ions in D_2O induce a very different behavior than ions in H_2O, without displaying any ion specificity. All of this implies that bulk water itself and in particular hydrogen bonding is crucial in the explanation of the observed differences in Fig. 5. In addition, Fig. 5B shows that there is a substantial difference between the fs-ESHS response of H_2O solvated and D_2O solvated electrolyte solutions. More specifically, the onset for the intensity rise along with the saturation concentration shift to higher electrolyte concentrations by a factor of ~6. Both data in Fig. 5B is normalized to clearly demonstrate this 6 × difference. This substantial shift verifies that the observed bulk response is, indeed, due to the change in the orientational order of water network, and not due to the individual ions.

Comparing the SH data from the surface and the bulk of Fig. 5, it can be seen that the bulk water SH intensity changes occur at much lower concentrations than the surface ion SH intensity changes. It is also noteworthy that both curves can be described by a Langmuir equation, even though only one of the SH data sets reports on a surface phenomenon. Clearly, the fact that the data follows the functional form of a Langmuir isotherm is no guarantee that a surface process is involved. Interestingly, the fs-ESHS intensity saturation concentrations for both H_2O and D_2O match with the surface tension minimum of the Jones-Ray effect as seen in Figs. 2B and 5B. Thus, adding electrolytes to water results in an increase in the orientational ordering of water molecules. This increase arises from the response of the hydrogen bond network of water to the total electrostatic field of the ions. Such behavior can be qualitatively described by a function that is identical to the Langmuir isotherm, and can be derived from Debye-Hückel theory (Refs. [33,63]). The increase in the overall alignment of water molecules causes a slight increase in the free energy or chemical potential of the bulk water in the dilute electrolyte concentration, but the change is very small as the observed increase in alignment is also very small. In what follows we connect this interpretation of recent data to thermodynamic and electrostatic models of the surface tension that have been recently published.

3.3. Connecting second harmonic and surface tension data

The surface tension can be defined as the surface excess Gibbs or Helmholtz energy, $\gamma = G_a^\sigma = H_a^\sigma - TS_a^\sigma$ with $G_a^\sigma, H_a^\sigma, T, S_a^\sigma$ the Gibbs energy, enthalpy, absolute temperature and entropy [64]. Here the subscript a denotes the area and σ indicates that the surface excess is given with respect to water. Under conditions of constant volume and pressure, for a 1:1 electrolyte dissolved in water, that is considered as an electroneutral species (indicated by s) we also have the Gibbs equation [25,64]:

$$d\gamma = -S_a^\sigma dT - \Gamma_s d\mu_s \tag{4}$$

which defines S_a^σ and Γ_s as:

$$S_a^\sigma = -\left(\frac{d\gamma}{dT}\right)_{\mu_s} \tag{5}$$

$$\Gamma_s = -\left(\frac{d\gamma}{d\mu_s}\right)_T \tag{6}$$

with μ_s the chemical potential of electrolyte s defined as a function of solute partial concentration (x_s) and activity coefficient f_s:

$$\mu_s = \mu_s^\circ + RT(f_s x_s). \tag{7}$$

The chemical potential μ_s reflects the free energy change of the system when a single electrolyte pair is added to the solution. It represents the sum of all intermolecular interactions associated with s. μ_s° represents the chemical potential for a reference state (a solution that behaves ideally at infinite dilution) [64].

Drzymala and Lyklema [25], considered the temperature dependence of the surface tension and used it to show that γ can be expressed as follows:

$$\gamma = H_a^\sigma + T\left[\left(\frac{d\gamma}{dT}\right)_{x_s} + \frac{1}{2RT}\left(\frac{\partial\gamma}{\partial\ln(f_s x_s)}\right)_T\left(S_s^\circ - 2R\ln(f_s x_s) - 2RT\left(\frac{\partial\ln(f_x)}{\partial T}\right)_{x_s}\right)\right. \tag{8}$$

where S_s° is the entropy of hydration, which is a bulk property. The enthalpic term in this expression contains the unfavorable interactions with the surface region, for example as contained in the image charge expression by Onsager and Samaras. Eq. (8) also illustrates that a decrease in the hydration entropy as induced by an increase in the orientational order of hydrating water molecules in between ions decreases the surface tension, providing a connection with the discussed ion induced solvent changes of section II. The minimum observed in Fig. 1B and Fig. 2B derives from a response of the solute (water) to the combined electric field of the ions. The behavior observed in Figs. 1 and 2 can then be ascribed to the interplay of two interactions: The influence of the electric field of the ions on the water-water interactions, which is dominant at micro- to low millimolar salt concentrations that results in a lowering of the surface tension and relates to the entropic term of Eq. (8). The unfavorable interactions of ions with the interfacial region, due to ion-dipole interactions, polarizability and hydrogen bonding, cause an increase in the interfacial tension and become apparent at concentrations around 50 mM.

In addition to the above discussion based on the second harmonic experiments of section II, several recent theoretical works have applied field theories to find expressions for the concentration dependence of the surface tension [65–67]. In these theories, γ is determined by the change in the purely electrostatic free energy of the solutions when a dielectric boundary is introduced. $\gamma(x_s)$ is given as a sum of two terms. A first term, due to the repulsion of ions by the interface, as described in the Onsager-Samaras model by an unfavorable interaction between an ion and its image charge induced by the dielectric boundary [1]. A second term is due to the induced polarization of the surrounding dielectric by the mean electric field of all the ions. As this field is stronger for higher concentrations, the dielectric is more stabilized: this interaction leads to a functional form for the surface tension of $-A\sqrt{x_s}$, where A is a constant. This contribution to the surface tension decreases with increasing x_s. This second term has been ignored in some theoretical works in which only the high-concentration behavior was studied [66], but is required to give a full picture of the concentration dependence of γ, which leads to the observed behavior in Fig. 1 and 2.

As these treatments of Refs. [65–67] are considering only purely electrostatic interactions, they can provide only a qualitative understanding of the behavior of $\gamma(x_s)$. More specifically, they are not sophisticated enough to explain the significant isotope effect observed, but do illustrate that the minimum in Fig. 1B and Fig. 2B is due to the response of the solvent to the combined electric field of the ions. This treatment is consistent with the treatment of Drzymala and Lyklema summarized in Eq. (8). To capture the isotope effect observed in Fig. 2B more sophisticated modelling has to be performed, with more realistic water models. Thus, qualitatively the minimum in the surface tension can be explained by the interplay of two major mechanisms: firstly, the influence of the ions' electric field on the interactions between water molecules (described in field theories by the energy stored in the dielectric medium surrounding the ions, used as a model of the solvent), which is dominant at micro to low millimolar salt concentrations and results in a lowering of the surface tension. Secondly, the unfavorable interactions of ions with the interfacial region due to ion-dipole interactions, polarizability and hydrogen bonding (described by the repulsion between ions and their image charges), causes an increase in the interfacial tension and becoming apparent at concentrations around 50 mM.

4. Conclusions

In this work, we have proposed and discussed the underlying mechanism for the Jones-Ray effect, the surface tension minimum at ~1–2 mM aqueous electrolyte concentrations. First, various concerns about the validity of the Jones-Ray measurements in the late 1930s and the recent reproduction of these results were addressed. More specifically, the influence of organic impurities, carbonic acid formation from CO_2(g) in ambient air, and the role of the substrate, i.e. the Pt Wilhelmy plate, were tested. Explicit measurements were performed to address these concerns and their influences were shown to be minimal if there were any. Thus, the Jones-Ray effect is not an experimental artifact and relates to the interactions of ions with water. However, the conventionally proposed mechanism based on ion adsorption to a phenomenological rare binding site at the air/water interface was considered difficult to reconcile with the provided data. Instead, the underlying mechanism for the observed surface tension minimum was discussed in light of recent non-resonant bulk water and ion resonant surface second harmonic experiments. We propose that the surface tension minimum originates from bulk ion-induced water-water correlations rather than ion adsorption at the interface. As ions are added to water, the hydrogen bond network of water responds to the collective electrostatic field of ions by increasing its orientational order. This increase in orientational order gives rise to an entropic penalty, which causes a reduction in the surface tension. The proposed mechanism agrees with surface tension measurements of NaCl solutions in H_2O and D_2O, bulk non-resonant second harmonic scattering experiments that probe the orientational order of water in the same solutions, and surface ion resonant second harmonic reflection experiments that probe the interfacial population of the anions and does not require the presence of a rare binding site. In addition, we show that recently published thermodynamic and purely electrostatic treatments of the surface tension as a function of electrolyte concentration do provide support for this interpretation as the surface tension also relies on the hydration entropy of ions and the electrostatic interactions contain two counter-acting contributions to the surface tension.

Acknowledgements

We thank Eric Tyrode for discussions and Zhi Luo, and Gianluca Etienne for their help with the contact angle measurements. This work is supported by the Julia Jacobi Foundation, the Swiss National Science Foundation and the European Research Council (grant number 616305). D.M.W. acknowledges funding from the Swiss National Science Foundation (Project ID 200021163210).

References

[1] L. Onsager, N.N.T. Samaras, The Surface Tension of Debye-Hückel Electrolytes, J. Chem. Phys. 2 (8) (1934) 528–536.
[2] C. Wagner, The surface tension of diluted electrolyte solutions, Physikalische Zeitschrift 25 (1924) 474–477.
[3] N.L. Jarvis, M.A. Scheiman, Surface potentials of aqueous electrolyte solutions, J. Phys. Chem. 72 (1) (1968) 74–78.
[4] L.M. Pegram, M.T. Record, Hofmeister salt effects on surface tension arise from partitioning of anions and cations between bulk water and the air−water interface, J. Phys. Chem. B 111 (19) (2007) 5411–5417.
[5] H.I. Okur, J. Hladílková, K.B. Rembert, Y. Cho, J. Heyda, J. Dzubiella, P.S. Cremer, P. Jungwirth, Beyond the Hofmeister series: ion-specific effects on proteins and their biological functions, J. Phys. Chem. B 121 (9) (2017) 1997–2014.
[6] N. Agmon, H.J. Bakker, R.K. Campen, R.H. Henchman, P. Pohl, S. Roke, M. Thämer, A. Hassanali, Protons and hydroxide ions in aqueous systems, Chem. Rev. 116 (13) (2016) 7642–7672.
[7] N. Schwierz, D. Horinek, R.R. Netz, Anionic and cationic hofmeister effects on hydrophobic and hydrophilic surfaces, Langmuir 29 (8) (2013) 2602–2614.
[8] R. Scheu, Y. Chen, M. Subinya, S. Roke, Stern layer formation induced by hydrophobic interactions: a molecular level study, J. Am. Chem. Soc. 135 (51) (2013) 19330–19335.
[9] K.B. Rembert, J. Paterova, J. Heyda, C. Hilty, P. Jungwirth, P.S. Cremer, Molecular mechanisms of ion-specific effects on proteins, J. Am. Chem. Soc. 134 (24) (2012) 10039–10046.
[10] X. Chen, T. Yang, S. Kataoka, P.S. Cremer, Specific ion effects on interfacial water structure near macromolecules, J. Am. Chem. Soc. 129 (40) (2007) 12272–12279.
[11] P.B. Petersen, R.J. Saykally, Probing the interfacial structure of aqueous electrolytes with femtosecond second harmonic generation spectroscopy, J. Phys. Chem. B 110 (29) (2006) 14060–14073.
[12] P. Jungwirth, D.J. Tobias, Specific ion effects at the air/water interface, Chem. Rev. 106 (4) (2006) 1259–1281.
[13] P.B. Petersen, R.J. Saykally, Adsorption of ions to the surface of dilute electrolyte solutions: the Jones-Ray effect revisited, J. Am. Chem. Soc. 127 (44) (2005) 15446–15452.
[14] P.B. Petersen, J.C. Johnson, K.P. Knutsen, R.J. Saykally, Direct experimental validation of the Jones-Ray effect, Chem. Phys. Lett. 397 (1–3) (2004) 46–50.
[15] P. Jungwirth, D.J. Tobias, Ions at the air/water interface, J. Phys. Chem. B 106 (25) (2002) 6361–6373.
[16] S. Enami, H. Mishra, M.R. Hoffmann, A.J. Colussi, Hofmeister effects in micromolar electrolyte solutions, J. Chem. Phys. 136 (15) (2012) 154707.
[17] S. Gopalakrishnan, D.F. Liu, H.C. Allen, M. Kuo, M.J. Shultz, Vibrational spectroscopic studies of aqueous interfaces: Salts, acids, bases, and nanodrops, Chem. Rev. 106 (4) (2006) 1155–1175.
[18] R. Scheu, B.M. Rankin, Y. Chen, K.C. Jena, D. Ben-Amotz, S. Roke, Charge asymmetry at aqueous hydrophobic interfaces and hydration shells, Angew. Chem. Int. Ed. 53 (36) (2014) 9560–9563.
[19] Y. Levin, A.P. dos Santos, A. Diehl, Ions at the air-water interface: an end to a hundred-year-old Mystery?, Phys Rev. Lett. 103 (25) (2009) 257802.
[20] P.B. Petersen, R.J. Saykally, On the nature of ions at the liquid water surface, In Annu. Rev. Phys. Chem. 57 (2006) 333–364.
[21] L.M. Pegram, M.T. Record, Thermodynamic Origin of Hofmeister Ion Effects, J. Phys. Chem. B 112 (31) (2008) 9428–9436.
[22] T.P. Pollard, T.L. Beck, Toward a quantitative theory of Hofmeister phenomena: from quantum effects to thermodynamics, Curr. Opin. Colloid Interface Sci. 23 (2016) 110–118.
[23] P. Lo Nostro, B.W. Ninham, Hofmeister Phenomena: An Update on Ion Specificity in Biology, Chem. Rev. 112 (4) (2012) 2286–2322.
[24] D. Horinek, R.R. Netz, Specific ion adsorption at hydrophobic solid surfaces, Phys. Rev. Lett. 99 (22) (2007) 226104.
[25] J. Drzymala, J. Lyklema, Surface Tension of Aqueous Electrolyte Solutions. Thermodynamics, J. Phys. Chem. A 116 (25) (2012) 6465–6472.
[26] D.E. Otten, P.R. Shaffer, P.L. Geissler, R.J. Saykally, Elucidating the mechanism of selective ion adsorption to the liquid water surface, Proc. Natl. Acad. Sci. 109 (3) (2012) 701–705.
[27] G. Jones, W.A. Ray, The surface tension of solutions, J. Am. Chem. Soc. 57 (5) (1935) 957–958.
[28] G. Jones, W.A. Ray, The surface tension of solutions of electrolytes as a function of the concentration I A differential method for measuring relative surface tension, J. Am. Chem. Soc. 59 (1937) 187–198.
[29] G. Jones, W.A. Ray, The surface tension of solutions of electrolytes as a function of the concentration. III. Sodium chloride, J. Am. Chem. Soc. 63 (1941) 3262–3263.
[30] G. Jones, W.A. Ray, The surface tension of solutions of electrolytes as a function of the concentration. IV. Magnesium sulfate, J. Am. Chem. Soc. 64 (1942) 2744–2745.
[31] G. Jones, W.A. Ray, The surface tension of solutions of electrolytes as a function of the concentration. III. Sodium chloride, J. Am. Chem. Soc. 63 (12) (1941) 3262–3263.
[32] M. Dole, J.A. Swartout, A twin-ring surface tensiometer. I. The apparent surface tension of potassium chloride solutions, J. Am. Chem. Soc. 62 (1940) 3039–3045.
[33] Y. Chen, H.I. Okur, N. Gomopoulos, C. Macias-Romero, P.S. Cremer, P.B. Petersen, G. Tocci, D.M. Wilkins, C. Liang, M. Ceriotti, S. Roke, Electrolytes induce long-range orientational order and free energy changes in the H-bond network of bulk water, Sci. Adv. 2 (4) (2016) e1501891.
[34] V. Venkateshwaran, S. Vembanur, S. Garde, Water-mediated ion–ion interactions are enhanced at the water vapor–liquid interface, Proc. Nat. Acad. Sci. United States Am. 111 (24) (2014) 8729–8734.
[35] I. Langmuir, Repulsive forces between charged surfaces in water, and the cause of the Jones-Ray effect, Science 88 (1938) 430–432.
[36] I. Langmuir, The role of attractive and repulsive forces in the formation of tactoids, thixotropic gels, protein crystals and coacervates, J. Chem. Phys. 6 (12) (1938) 873–896.
[37] H.M. Cassel, Jones-Ray effect, wettability, and zeta-potential, J. Chem. Phys. 14 (7) (1946) 462.
[38] A.S. Coolidge, Imaginary Contact Angles and the Jones-Ray Effect, J. Am. Chem. Soc. 71 (6) (1949) 2153–2167.
[39] F.A. Long, G.C. Nutting, The Relative Surface Tension of Potassium Chloride Solutions by a Differential Bubble Pressure Method1, J. Am. Chem. Soc. 64 (10) (1942) 2476–2482.
[40] G. Passoth, Uber den Jones-Ray-effekt und die Oberflächenspannung verdünnter elektrolytlosungen, Z. Physik. Chem 211 (1959) 129.
[41] A.W. Adamson, A.P. Gast, Physical chemistry of surfaces, Sidney, Wiley-interscience, 1997.
[42] M. Dole, A theory of surface tension of aqueous solutions, J. Am. Chem. Soc. 60 (4) (1938) 904–911.
[43] P. Koelsch, H. Motschmann, Varying the counterions at a charged interface, Langmuir 21 (8) (2005) 3436–3442.
[44] P. Koelsch, H. Motschmann, A method for direct determination of the prevailing counterion distribution at a charged surface, J. Phys. Chem. B 108 (48) (2004) 18659–18664.
[45] P. Koelsch, H. Motschmann, An experimental route to Hofmeister, Curr. Opin. Colloid Interface Sci. 9 (1–2) (2004) 87–91.
[46] K.W. Bewig, W.A. Zisman, The wetting of gold and platinum by water, J Phys Chem-Us 69 (12) (1965) 4238–4242.
[47] R.R. Sowell, N.J. Delollis, H.J. Gregory, O. Montoya, Effect of Activated Gas Plasma on Surface Characteristics and Bondability of RTV Silicone and Polyethylene, J. Adhes. 4 (1) (1972) 15–24.
[48] Y. Markus, Ion Properties, Marcel Dekker, 1997.
[49] N. Gomopoulos, C. Lütgebaucks, Q. Sun, C. Macias-Romero, S. Roke, Label-free second harmonic and hyper Rayleigh scattering with high efficiency, Opt. Express 21 (1) (2013) 815–821.
[50] A.L. Sumner, E.J. Menke, Y. Dubowski, J.T. Newberg, R.M. Penner, J.C. Hemminger, L.M. Wingen, T. Brauers, B.J. Finlayson-Pitts, The nature of water on surfaces of laboratory systems and implications for heterogeneous chemistry in the troposphere, Phys. Chem. Chem. Phys. 6 (3) (2004) 604–613.
[51] P.M. Mukerjee, J. Karol, Critical micelle concentrations of aqueous surfactant solutions, 1971.
[52] N.J. Chang, E.W. Kaler, The structure of sodium dodecyl sulfate micelles in solutions of water and deuterium oxide, J. Phys. Chem. 89 (14) (1985) 2996–3000.
[53] J. Curry, C.L. Hazelton, The first thermodynamic ionization constant of deuterio-carbonic acid at 25°1, J. Am. Chem. Soc. 60 (11) (1938) 2773–2776.
[54] J. Curry, Z.Z. Hugus, The second ionization constant of deuterocarbonic acid, J. Am. Chem. Soc. 66 (4) (1944) 653–655.
[55] Boyd, R. W. Nonlinear Optics. 1992.
[56] J.C. Conboy, M.C. Messmer, G.L. Richmond, Dependence of alkyl chain conformation of simple ionic surfactants on head group functionality as studied by vibrational sum-frequency spectroscopy, J. Phys. Chem. B 101 (34) (1997) 6724–6733.
[57] J.T. O'Brien, J.S. Prell, M.F. Bush, E.R. Williams, Sulfate Ion Patterns Water at Long Distance, J. Am. Chem. Soc. 132 (24) (2010) 8248–8249.
[58] D.F. Parsons, M. Bostrom, P.L. Nostro, B.W. Ninham, Hofmeister effects: interplay of hydration, nonelectrostatic potentials, and ion size, Phys. Chem. Chem. Phys. 13 (27) (2011) 12352–12367.
[59] Y. Marcus, A simple empirical model describing the thermodynamics of hydration of ions of widely varying charges, sizes, and shapes, Biophys. Chem. 51 (2) (1994) 111–127.
[60] J.D. Smith, R.J. Saykally, P.L. Geissler, The effects of dissolved halide anions on hydrogen bonding in liquid water, J. Am. Chem. Soc. 129 (45) (2007) 13847–13856.
[61] P.R. Hünenberger, M. Reif, Single-ion solvation: experimental and theoretical approaches to elusive thermodynamic quantities. Royal society of chemistry: UK, 2011.
[62] A.J. Moad, G.J. Simpson, A unified treatment of selection rules and symmetry relations for sum-frequency and second harmonic spectroscopies, J. Phys. Chem. B 108 (11) (2004) 3548–3562.

[63] D.M. Wilkins, D.E. Manolopoulos, S. Roke, M. Ceriotti, Mean-field theory of water-water correlations in electrolyte solutions, J. Chem. Phys. 146 (18) (2017) 181103.
[64] E.A. Guggenheim, Thermodynamics: an advanced treatment for chemists and physicists. Elsevier Science Publishing Company, 1986.
[65] T. Markovich, D. Andelman, R. Podgornik, Surface tension of electrolyte interfaces: Ionic specificity within a field-theory approach, J. Chem. Phys. 142 (4) (2015) 044702.
[66] M. Tomer, A. David, P. Rudi, Surface tension of electrolyte solutions: a self-consistent theory, EPL (Europhysics Lett.) 106 (1) (2014) 16002.
[67] R. Wang, Z.-G. Wang, Effects of ion solvation on phase equilibrium and interfacial tension of liquid mixtures, J. Chem. Phys. 135 (1) (2011) 014707.

Halil I. Okur received his B.S. and M.Sc. degrees in Chemistry from Bilkent University (Turkey), followed by a Ph.D. in Chemistry at the Pennsylvania State University, working with Professor Paul S. Cremer. He is currently doing postdoctoral studies at the École Polytechnique Fédérale de Lausanne (EPFL), working with Professor Sylvie Roke. His research focuses on developing and performing experiments with biologically relevant interfaces to explain macroscopic properties with molecular level details. His current interests include elucidating specific ion interactions at various interfaces and characterizing lipid monolayer/membrane systems.

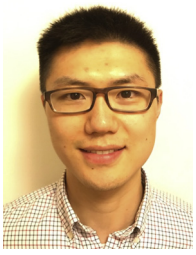

Yixing Chen obtained his B.S and B.Eng. degrees in Opto-electronics from Nankai University and Tianjin University (China), M.Sc. degree in Photonics from Jena University (Germany), and Ph.D. degree in Science from EPFL (Switzerland) under the supervision of Prof. Sylvie Roke. He is currently doing postdoctoral work in the group of Prof. Sylvie Roke. His research focuses on utilizing nonlinear spectroscopic methods and theoretical modeling to study molecular interactions in various aqueous systems including electrolyte solutions and nanoscale aqueous interfaces.

David M. Wilkins completed his M.Chem and D.Phil in Physical and Theoretical Chemistry at the University of Oxford (2012 and 2016) under the supervision of Prof. David Manolopoulos. He is currently carrying out postdoctoral work in the group of Prof. Michele Ceriotti at EPFL. His current research interests include path-integral simulations of nuclear quantum effects in aqueous systems, and the development of computational and theoretical techniques to understand nonlinear light scattering experiments.

Sylvie Roke obtained B.Sc. and M.Sc. degrees with highest honors in chemistry (2000) and physics (2000) from Utrecht University and a Ph.D. degree in natural sciences from Leiden University (2004, highest honors). In 2005 she was awarded an independent research group leader (W2) position by the Max Planck Society. In 2011 she moved to EPFL, where she holds the Juli Jacobi chair in photomedicine. She received the Minerva Prize (2006), the Hertha Sponer Prize (2008), an ERC Starting Grant (2009), and an ERC Consolidator Grant (2014). Her research focuses on understanding aqueous systems, interfaces, soft matter, and biological systems by using and developing a variety of novel spectroscopic and imaging methods.